Scale-Free Intermittent Flow in Crystal Plasticity

Dennis M. Dimiduk,[1]* Chris Woodward,[2] Richard LeSar,[3] Michael D. Uchic[1]

Under stress, crystals irreversibly deform through complex dislocation processes that intermittently change the microscopic material shape through isolated slip events. These underlying processes can be revealed in the statistics of the discrete changes. Through ultraprecise nanoscale measurements on nickel microcrystals, we directly determined the size of discrete slip events. The sizes ranged over nearly three orders of magnitude and exhibited a shock-and-aftershock, earthquake-like behavior over time. Analysis of the events reveals power-law scaling between the number of events and their magnitude, or scale-free flow. We show that dislocated crystals are a model system for studying scale-free behavior as observed in many macroscopic systems. In analogy to plate tectonics, smooth macroscopic-scale crystalline glide arises from the spatial and time averages of disruptive earthquake-like events at the nanometer scale.

The vivid images of radiant-hot metal being forged on a blacksmith's anvil, or being formed between rolls and dies, support a view of crystal deformation as analogous to viscous fluid flow. Such deformation is often described via a set of continuum-level parameters, which, in contrast to those describing fluids, evolve with deformation to reflect the increasing resistance to flow that occurs with increasing distortion (work hardening). Although continuum approaches are selectively useful for describing deformation, especially at high temperatures, they completely fail to account for well-known intermittent deformation phenomena such as the spatial localization of dislocation flow into "slip bands" [described in 1900 (*1*)] and the temporal fluctuations in load-versus-time curves (the Portevin–Le Chatelier effect first reported in the 1920s) (*2*, *3*).

From the late 1950s to the 1970s, numerous investigators sought to account for the heterogeneous nature of crystal deformation. Studies ranged from examining the motion of individual dislocations to describing the development and propagation of dislocation aggregates to form deformation bands (*4*). Those studies demonstrated the importance of both topological (crystallographic) constraints and the complex, long-range interactions between dislocations that determine collective dislocation motion, thus distinguishing crystal plasticity from continuum flow. For example, Pond convincingly showed that crystal slip in metals can be intermittent and heterogeneous at multiple length and time scales through cinematographic studies of deformation band formation and growth (*5*). Studies of dislocation motion, slip-line formation, and the collective intermittent nature of slip continued, providing a detailed view of dislocation motion and crystal glide (*6*–*8*). Despite much effort, a quantitative understanding of intermittency and collective dislocation flow has remained elusive. As a consequence, our ability to predict critical deformation behavior is often limited, impeding our understanding of such phenomena as work hardening (*9*–*11*).

Recent studies of intermittency in crystal plasticity were based on measurements of acoustic emissions that arise from the motion of dislocations through large (tens to hundreds of mm) ice crystals (*12*–*16*). The essence of the technique is the detection of the acoustic waves that are generated by dislocation glide and their subsequent analysis based on models of dislocation motion. Under some conditions, it has been argued that the amplitudes of the acoustic signals are related to the area swept by the fast-moving dislocations and hence to the energy dissipated during deformation events. These results were used to suggest intermittency of flow (*12*), scale-free dissipation processes (*13*), spatial clustering of flow avalanches (*14*), and, most recently, conditions for "supercritical" flow in polycrystalline ice (*15*, *16*). However, the results from these measurements can only be interpreted via models and under certain key assumptions about the deformation processes. Other reports also show the characteristics of scale-free flow for crystals through simulation (*17*–*19*) and models of dislocation glide at low temperature (*20*, *21*). These studies conclude that deformation of crystals having highly mobile dislocations exhibits the attributes of a self-organized critical (SOC) process.

We report the direct measurement of scale-free intermittent flow within micrometer-scale pure metal crystals loaded above the elastic-plastic transition. Using the ultrahigh displacement resolution offered by modern nanoindentation systems (effectively a nanoscale seismometer), we examined the frequency of displacement events as a function of their magnitude for several sample sizes and applied loads. The results were analyzed following the suggestion that dislocations form a SOC system, as briefly reviewed in (*22*, *23*). Bak *et al*. (*24*) introduced this concept to describe dynamical systems that arrange themselves such that they are always at a critical point irrespective of their initial state, that is, they self-organize to the critical point of the system (*25*). An important aspect of SOC behavior is that it is self-similar or scale-free. That is, structures at one scale appear the same (at least in a statistical sense) as structures at other scales. If dislocations are indeed self-organized critical systems, then the statistics that describe these ensembles can be used to develop homogenization schemes for mapping between groups of dislocations and macroscopic deformation.

The experimental techniques used for this study were reported in (*26*–*28*) [see also (*29*)]. Microcrystals of pure Ni were prepared by isolating cylindrical columns via focused ion-beam machining, with one end of each column attached to the bulk material, within the surface of an electropolished macroscopic crystal. The microcrystals were transferred to a nanoindenter and aligned for axial compression testing. Samples ranging in diameter from 18 to 30.7 μm, with length-to-diameter ratios ranging from ~1.9:1 to 2.8:1, were loaded via a flattened diamond tip platen at a nominal axial strain rate of 10^{-4}/s at room temperature. For each sample a variety of parameters were measured, including load (±50 nN) and displacement (±0.02 nm), and digitally stored at a frequency of 5 Hz. The displacement-versus-time data were differentiated by a simple two-point forward-derivative method. The resultant loading platen velocity profiles were correlated with the displacement-versus-time data to identify displacement events larger than a chosen "noise threshold." The shear-stress versus shear-strain curves measured for the present experiments and a typical plot of detected displacements versus time are shown in Fig. 1, A and B. Note that the displacements reflect dissipated energy and are intermittent in both space and time, despite the programmed continuous loading rate.

For the scaling analysis, a noise threshold for detecting displacements was established for each test by monitoring the standard deviation from ideal of the detected displacements during the unloading portion of the test. For these tests, the noise values ranged from 0.13 to 0.68 nm. Thus, for Ni crystals with ⟨–2, 6, 9⟩ orientation, a typical minimum detected event corresponds to ~0.3 nm or ~4 dislocations leaving the crys-

[1]Air Force Research Laboratory, Materials and Manufacturing Directorate, AFRL/MLLM, Wright-Patterson AFB, OH 45433, USA. [2]Department of Materials Science and Engineering, Northwestern University, Evanston, IL 60208, USA. [3]Theoretical Division, Los Alamos National Laboratory, Los Alamos, NM 87545, USA.

*To whom correspondence should be addressed. E-mail: dennis.dimiduk@wpafb.af.mil

tal. For events exceeding the noise threshold, the displacement magnitude was recorded and sorted into bins for each sample as well as for the collective set of samples. A plot of the number of events at a given displacement magnitude, $n(x)$, versus magnitude x (in nm) for events isolated from a single sample (Fig. 2) reveals that a linear regime exists in which the probability of observing a displacement event of a given magnitude decreases as the event size increases. Also shown in Fig. 2 are the displacements for all of the samples analyzed collectively. Both data sets demonstrate power-law scaling. The data were fit to a power-law expression $n(x) = Cx^{-\alpha}$, producing a measured value of $\alpha = \sim1.5$ where C is a constant. This scale-free flow was observed over a range of displacements from ~0.5 nm to more than ~150 nm per event—more than two orders of magnitude. Values for α derived from log-log plots are known to underestimate this parameter. Using alternative approaches as suggested by Newman (*25*), we estimated a power-law slope of 1.60 ± 0.02 by a bootstrap method (*29*). Note that the value of 1.6 is identical to that found through acoustic emission experiments (*13*) and from theory (*19*). Further, the scaling relationship is independent of sample size over the range examined as well as the gradually increasing stress over the range of the test (i.e., there is no work-hardening effect for single slip-plane flow).

Closer inspection of a typical sequence of events (Fig. 3) shows several important features of the data. First, the individual events take place at a rate that is much faster than the programmed displacement rate of the test. This demonstrates that dissipation is much faster than the rate of change of the driving force. Second, the largest displacement events typically occur after an increment of the remote stress. Note that the magnitude of a stress increment is a vanishingly small percentage of the total applied stress. This observation of "large" events (displacement shocks) after a small change of driving force indicates that the system is near critical. Third, these large events are frequently followed by a succession of additional displacement events of much smaller magnitude (aftershocks) that occur in the absence of further detectable remote stress rise; this suggests self-organization back to a critical state. Fourth, a post mortem examination of the deformed samples by transmission electron microscopy (TEM) (Fig. 4) shows a substructure containing many dislocations that is characteristic of those seen after similar deformation of large Ni crystals (*28*, *30*, *31*). Finally, the displacement-versus-time plots show intervals having a small positive slope that indicates additional displacements not accounted for within the detected bursts. These extra displacements occur even under conditions of no increase in the applied load, consistent with these samples exhibiting creep at or near criticality.

Our data and analysis explicitly show that crystalline glide in metals exhibits the characteristic attributes of self-organized criticality under the appropriate control of the driving force (in this case an applied displacement rate or load). These results support an emerging view that a statistical framework that creates a coarse-grained description of dislocation response is needed to bridge the

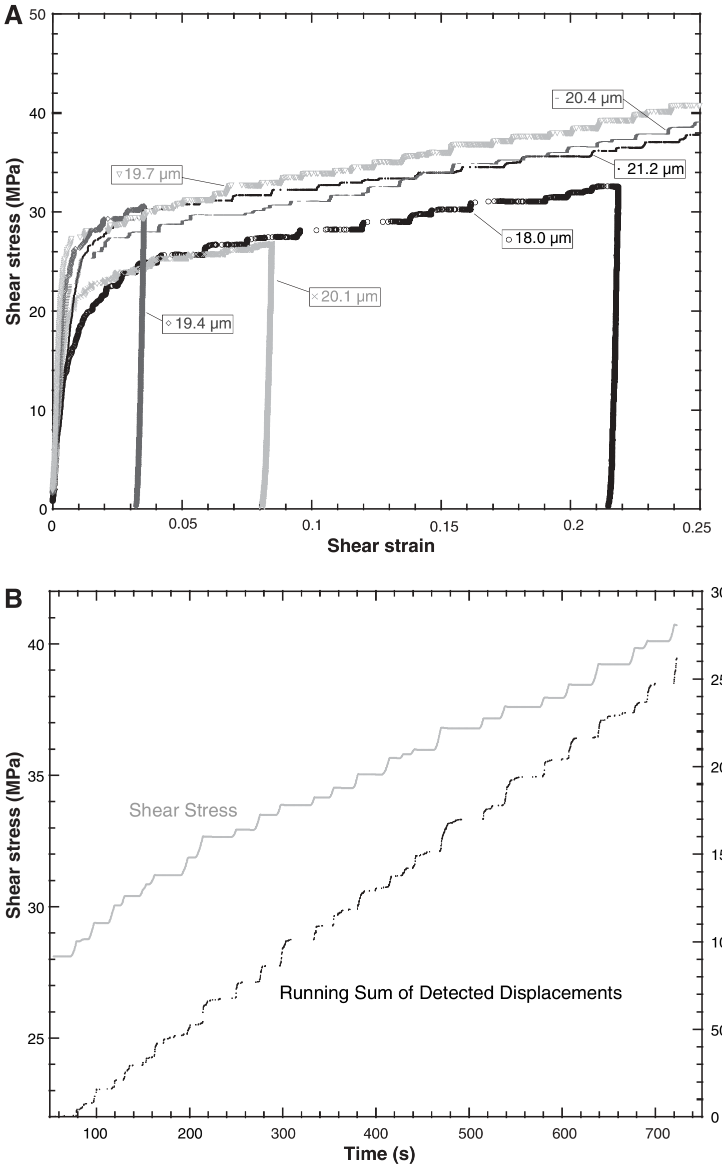

Fig. 1. (**A**) Selected shear-stress versus shear-strain curves for Ni samples with ⟨–2, 6, 9⟩ orientation, ~20 μm in diameter, showing intermittency of strain and stress. (**B**) Plot of shear stress and the cumulative sum of detected displacements as functions of time for a single sample 19.7 μm in diameter. See (*29*) for additional sample data from these and from samples ~30 μm in diameter.

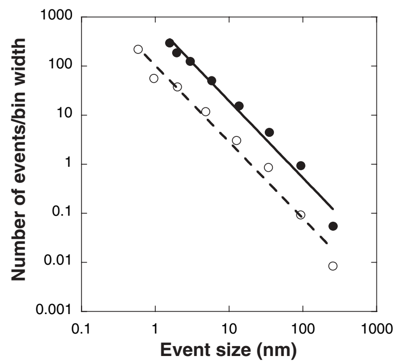

Fig. 2. Event frequency distribution showing the number of slip events of a certain size, $n(x)$, versus event size, x, plotted on logarithmic scales. Power-law scaling over more than two orders of magnitude is exhibited for both a single sample ~20 μm in diameter (open circles and dashed line fit) and the aggregate data from several samples (solid circles and solid line fit).

gap between the behavior of individual dislocations and the ensemble of dislocations that govern macroscopic metal plasticity. Further, the existence of a scale-free set of variables that describe deformation suggests that such a coarse-graining variable set exists (*23*). This assessment puts dislocation motion in the same class as earthquakes, sand pile avalanches, magnetic domain dynamics, and a wide variety of other dynamical systems. The picture that emerges is that crystal deformation has more in common with plate tectonics than with viscous fluid flow, at least in selected commonly experienced regimes.

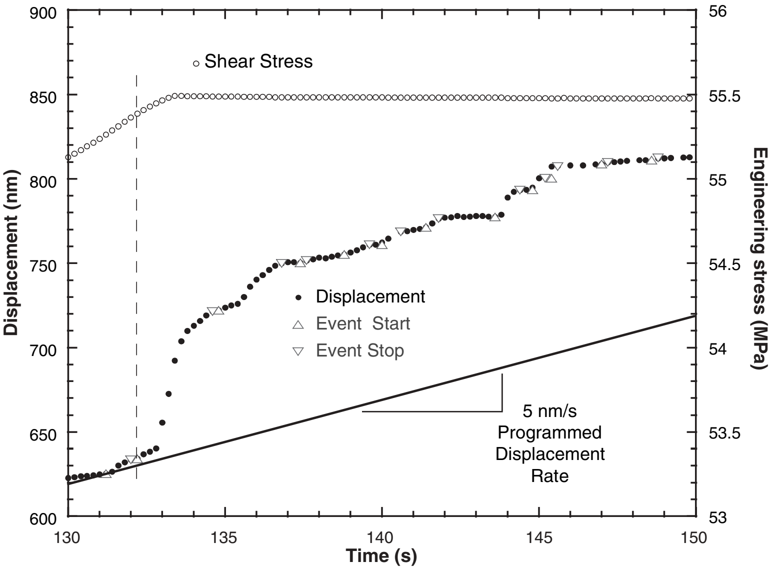

Fig. 3. A detailed example of the stress-versus-time and displacement-versus-time curves taken from the data for the sample 30.7 μm in diameter. The displacement curve shows superimposed markers for detected event start and stop times. Note that the large event beginning at the vertical dashed line occurs as a shock under a rising stress but continues under constant stress, as do the vast number of aftershocks at smaller magnitudes.

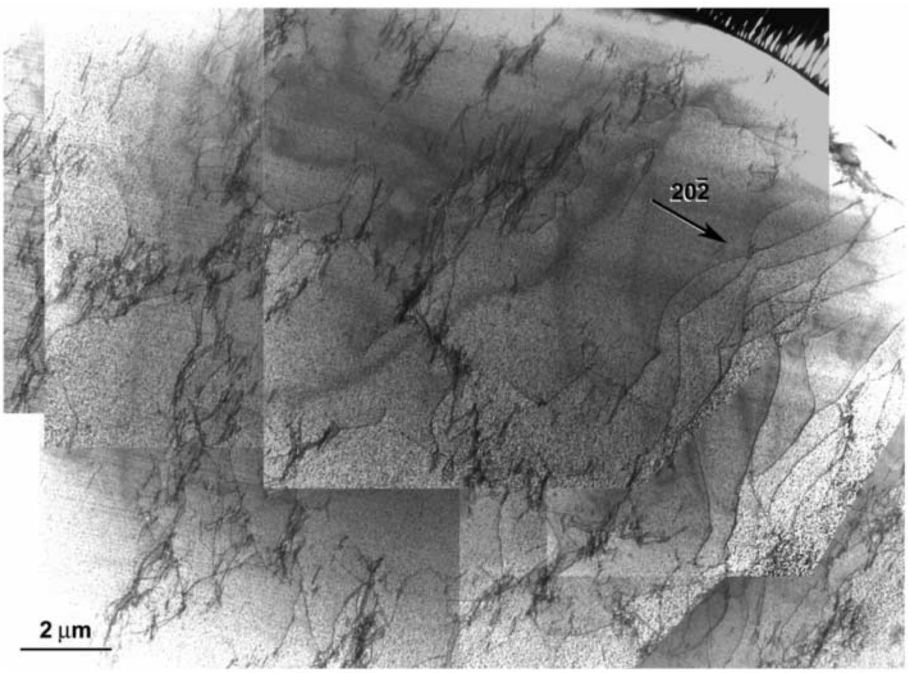

Fig. 4. Bright-field TEM image showing the dislocation structure for the sample 20.1 μm in diameter after 8.1% plastic shear strain. The plane of view is parallel to the {111} slip planes, and the field of view includes most of the sample cross section. The crystallographic direction marker indicates both the imaging vector and the direction of the dislocation Burgers vector. The montage image was digitally assembled from seven individually leveled micrographs, the edges of which can be seen.

References and Notes

1. J. A. Ewing, W. Rosenhain, *Philos. Trans. R. Soc. London Ser. A* **193**, 353 (1900).
2. A. Portevin, F. Le Chatelier, *C. R. Acad. Sci.* **176**, 507 (1923).
3. M. A. Lebyodkin, Y. Estrin, *Acta Mater.* **53**, 3403 (2005).
4. J. J. Gilman, in *Micromechanics of Flow in Solids* (McGraw-Hill, New York, 1969), pp. 185–199.
5. R. B. Pond, in *The Inhomogeneity of Plastic Deformation* (American Society for Metals, Metals Park, OH, 1973), pp. 1–18.
6. H. Neuhauser, in *Dislocations in Solids* (North-Holland, Amsterdam, 1983), vol. 6, pp 319–440.
7. E. M. Nadgorny, *Prog. Mater. Sci.* **31**, 434 (1988).
8. M. Zaiser, F. Madani, V. Koutos, E. C. Aifantis, *Phys. Rev. Lett.* **93**, 195507 (2004).
9. R. Madec, B. Devincre, L. Kubin, T. Hoc, D. Rodney, *Science* **301**, 1879 (2003).
10. P. Gumbsch, *Science* **301**, 1857 (2003).
11. A. H. Cottrell, in *Dislocations in Solids* (North-Holland, Amsterdam, 2002), vol. 11, pp. vii–xvii.
12. J. Weiss, J.-R. Grasso, *J. Phys. Chem. B* **101**, 6113 (1997).
13. M.-C. Miguel, A. Vespignani, S. Zapperi, J. Weiss, J.-R. Grasso, *Nature* **410**, 667 (2001).
14. J. Weiss, D. Marsan, *Science* **299**, 89 (2003).
15. T. Richeton, J. Weiss, F. Louchet, *Nat. Mater.* **4**, 465 (2005).
16. T. Richeton, J. Weiss, F. Louchet, *Acta Mater.* **53**, 4463 (2005).
17. M. Koslowski, R. LeSar, R. Thomson, *Phys. Rev. Lett.* **93**, 125502 (2004).
18. M. Koslowski, R. LeSar, R. Thomson, *Phys. Rev. Lett.* **93**, 265503 (2004).
19. M. Zaiser, P. Moretti, *J. Stat. Mech.*, 10.1088/1742-5468/2005/08/P08004 (2005).
20. I. Groma, F. F. Csikor, M. Zaiser, *Acta Mater.* **51**, 1271 (2003).
21. M.-C. Miguel, P. Moretti, M. Zaiser, S. Zapperi, *Mater. Sci. Eng. A* **400–401**, 191 (2005).
22. P. Sammonds, *Nat. Mater.* **4**, 425 (2005).
23. J. P. Sethna, K. A. Dahmen, C. R. Myers, *Nature* **410**, 242 (2001).
24. P. Bak, C. Tang, K. Wiesenfeld, *Phys. Rev. Lett.* **59**, 381 (1987).
25. M. E. J. Newman, *Contemp. Phys.* **46**, 323 (2005).
26. M. D. Uchic, D. M. Dimiduk, J. N. Florando, W. D. Nix, *Science* **305**, 986 (2004).
27. M. D. Uchic, D. M. Dimiduk, *Mater. Sci. Eng. A* **400–401**, 268 (2005).
28. D. M. Dimiduk, M. D. Uchic, T. A. Parthasarathy, *Acta Mater.* **53**, 4065 (2005).
29. See supporting material on *Science* Online.
30. S. Mader, in *Electron Microscopy and Strength of Crystals* (Interscience, New York, 1963), pp. 183–229.
31. J. Gil-Sevillano, in *Materials Science and Technology, Vol. 6, Plastic Deformation and Fracture of Materials* (Weinheim, New York, 1993), pp. 19–88.

32. We thank T. A. Parthasarathy and D. Trinkle for many useful discussions and for bringing reference (*25*) to our attention, and S. Polasik for the image of the dislocation structure in Fig. 4. Supported by the Defense Advanced Research Projects Agency and the Air Force Office of Scientific Research. The work of R.L. was performed under the auspices of the U.S. Department of Energy under contract W-7405-ENG-36.

Supporting Online Material
www.sciencemag.org/cgi/content/full/312/5777/1188/DC1
Materials and Methods
Figs. S1 to S4
Tables S1 and S2
References

15 December 2005; accepted 20 March 2006
10.1126/science.1123889

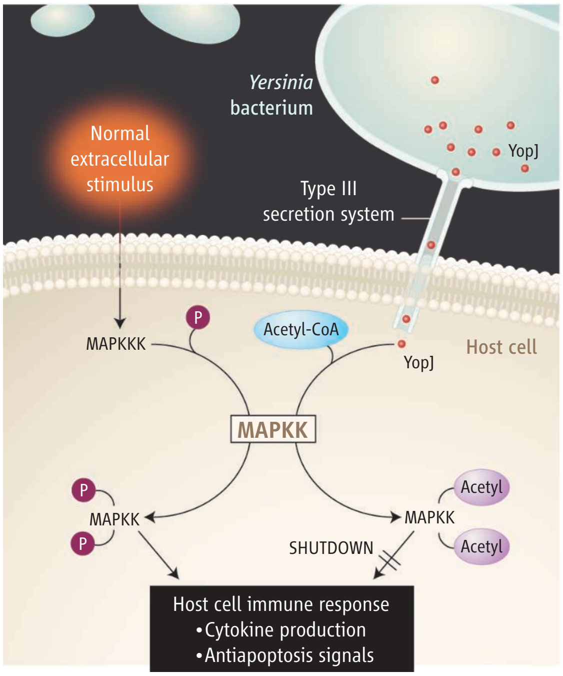

Virulence factor interference. YopJ that is deployed into a host cell blocks a signaling pathway by modifying the enzyme MAPK kinase (MAPKK) with acetyl moieties. This prevents activation of MAPKK by phosphorylation (P) via MAPKKK, and shuts down the immune response.

CREDIT: P. HUEY/SCIENCE

lar to a triad found in ClanCE cysteine proteases, which include AVP and the ubiquitin-like protease (Ulp-1) (*8*). Orth *et al*. (*7*) showed that YopJ can hydrolyze SUMO-1, a ubiquitin-like protein, from SUMO-1–conjugated proteins. Using a similar rationale, Zhou *et al*. (*9*) demonstrated that YopJ can function as a deubiquitinase. Neither of these observations, however, explains the ability of YopJ to specifically inhibit the MAPK pathways at the level of the MKKs. In light of the new data, it seems likely that the above observations may represent global cellular effects that can be obtained when a protein, usually expressed at low levels, is overexpressed in cells.

Mukherjee *et al.* show that YopJ is an acetyltransferase that blocks activation of the MAPK and NFκB pathways by acetylating serine and threonine residues on MKK6 and IKKβ. The authors used an in vitro system to recapitulate the ability of YopJ to inhibit the phosphorylation of MKK6. Subsequent analysis of MKK6 demonstrated that YopJ acetylates MKK6 on the serine or threonine residues critical for kinase activation, thus directly blocking its activation by phosphorylation. In addition, IKKβ is also acetylated on the two residues that are normally phosphorylated in its signaling cascade. Therefore, in each case, acetylation effectively blocks the ability of upstream kinases to phosphorylate and activate these proteins, thereby preventing the activation of downstream effectors. Although the details of the enzymatic posttranslational modification are yet to be worked out, most likely the cysteine residue of YopJ catalyzes the transfer of the acetyl group from acetyl-CoA to YopJ, forming an acyl enzyme intermediate. The acetylated form of YopJ then transfers the acetyl group to the reactive serine or threonine residues of MKK6 and IKKβ.

This activity for YopJ elegantly explains its ability to block phosphorylation of MKK6 and IKKβ and raises the interesting question of whether other MKKs present in parallel MAPK pathways also undergo similar modifications. This in turn raises other questions: Do other members of the YopJ family function as acetyltransferases? Do eukaryotic cells have acetyltransferases whose normal function is to regulate fluxes through the MAPK pathways, and do novel acetyltransferases exist to block sites of phosphorylation in other pathways? Hart and colleagues have suggested that glycosylation plays a similar role in blocking phosphorylation (*10*). Taken together, the direct competition of one posttranslational modification for another may be a more common cellular strategy for regulation of flux through signal transduction pathways than previously recognized.

Knowing that YopJ functions as an acetyltransferase is not the end of the story. It is really the beginning of what is likely to be the exciting search for other acetyltransferases in bacterial pathogens and viruses as well as in eukaryotic cells.

References

1. R. R. Brubaker, *Curr. Top. Microbiol. Immunol.* **57**, 111 (1972).
2. S. Mukherjee *et al.*, *Science* **312**, 1211 (2006).
3. L. E. Palmer, S. Hobbie, J. E. Galan, J. B. Bliska, *Mol. Microbiol.* **27**, 953 (1998).
4. L. E. Palmer, A. R. Pancetti, S. Greenberg, J. B. Bliska, *Infect. Immun.* **67**, 708 (1999).
5. K. Ruckdeschel *et al.*, *J. Exp. Med.* **187**, 1069 (1998).
6. K. Orth *et al.*, *Science* **285**, 1920 (1999).
7. K. Orth *et al.*, *Science* **290**, 1594 (2000).
8. A. J. Barrett, N. D. Rawlings, *J. Biol. Chem.* **382**, 727 (2001).
9. H. Zhou *et al.*, *J. Exp. Med.* **202**, 1327 (2005).
10. K. Kamemura, G. W. Hart, *Prog. Nucleic Acid. Res. Mol. Biol.* **73**, 107 (2003).

10.1126/science.1128785

MATERIALS SCIENCE

Fluctuations in Plasticity at the Microscale

M.-Carmen Miguel and Stefano Zapperi

During deformation, microscale materials may flow or change shape abruptly as atomic-scale defects migrate and assemble. The abrupt episodes of deformation appear to have a power-law distribution, a finding that may help in the design of miniature devices.

A fundamental challenge in materials science today is the investigation of size effects that influence the mechanical properties of micrometer- to nanometer-scale devices. These small scales are ubiquitous in modern technological applications and pose new theoretical questions as a result of the crucial role played by fluctuations. These fluctuations are observed as step changes or discontinuities in the mechanical response caused by the inhomogeneous dynamics of defects at the microscale. Fluctuations of this kind become more important as the size of any physical system decreases, hence they can lead to substantial deviations from the system's average behavior. On page 1188 of this issue, Dimiduk and co-workers (*1*) report experimental results on metal microcrystals that provide direct evidence of scale-invariant intermittent plastic flow—that is, permanent deformation with strain bursts that have a power-law distribution. These high-resolution experiments call for a novel theoretical framework that could help unravel microscopic deformation behavior in crystalline materials.

Plastic deformation is often described as a smooth process occurring in an elastic continuum. Yet microscopically it is due to the nucleation and motion of discrete crystal defects, known as dislocations. Dislocations self-assemble into intricate structures that determine the mechanical properties of a crystalline material. When external forces are applied, these dislocation structures dis-

M.-C. Miguel is in the Departament de Física Fonamental, Universitat de Barcelona, 08028 Barcelona, Spain. S. Zapperi is with the Consiglio Nazionale delle Ricerche–Istituto Nazionale per la Fisica della Materia, Dipartimento di Fisica, Università "La Sapienza," 00185 Roma, Italy. E-mail: stefano.zapperi@roma1.infn.it

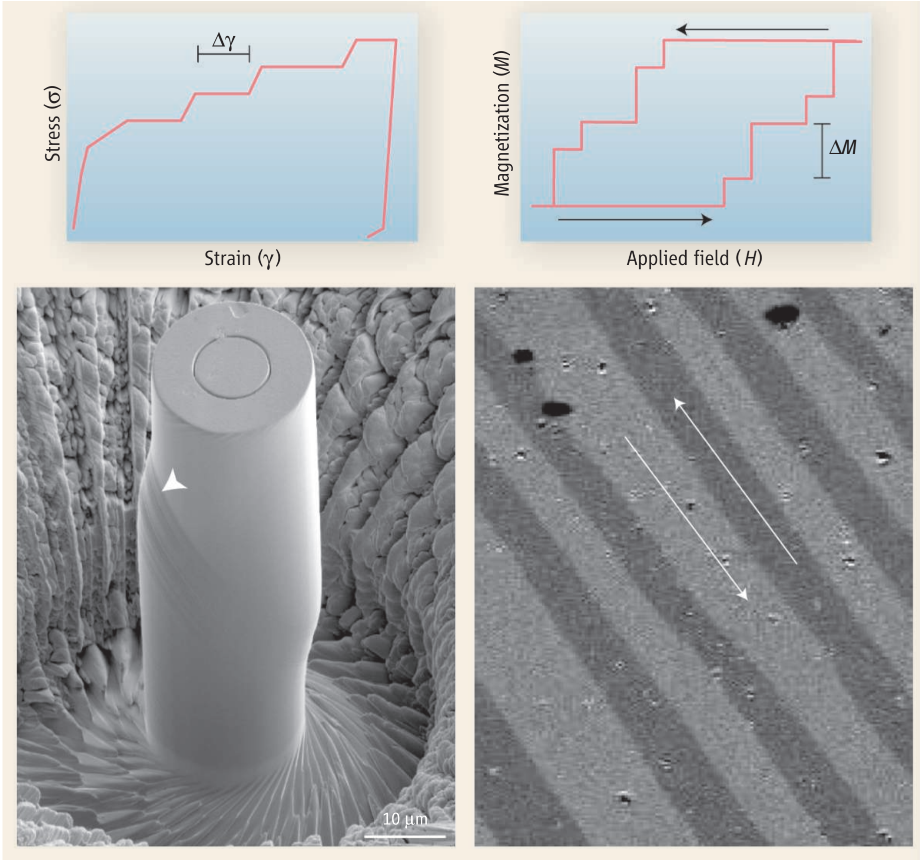

Plastic deformation of crystalline materials resembles ferromagnetic hysteresis. **(Top)** The bursts in a typical stress-strain curve from a micrometer-size sample **(left)** are analogous to the magnetization jumps in a hysteresis cycle of a ferromagnetic thin film **(right)**. **(Bottom left)** A cylindrical nickel sample after compression shows sloping slip planes (arrowhead) formed by motion of dislocations. **(Bottom right)** A magneto-optical image of a ferromagnetic alloy, where magnetization is due to the motion of domain walls (arrows).

entangle and become mobile, giving rise to plastic strain. Conventional analysis based on continuum models presumes that the microscopic details of this flow average out above a given size scale, so that fluctuations can safely be ignored.

The powerful experimental methodology developed by Dimiduk *et al*. and Uchic *et al*. (*2*) to manipulate small crystals challenges this viewpoint. Uniaxial compression testing of nickel crystals gives rise to staircase-like stress-strain curves (see the figure, top left) and, at the same time, leads to the formation of slip bands on the sample's surface (figure, bottom left), indicating dislocation-mediated deformation. Moreover, the yield stress, which separates elastic and plastic behavior, increases, as does its fluctuation, as the sample size is decreased (*2*). These experimental results exhibit some common features characteristic of other systems driven out of equilibrium. Bursts of activity (avalanches) and power law–distributed crackling noise are observed in a wide variety of physical systems, but, in particular, they are expected in the close vicinity of a critical point (*3*). Are all these mechanical observations thus interpretable within the realm of statistical mechanics, or more precisely, within the scenario of nonequilibrium phase transitions?

Dislocation dynamics models suggest that the onset of plasticity corresponds to a nonequilibrium phase transition, controlled by the external stress, that separates a jammed phase, in which dislocations are immobile, from a flowing phase (*4*). When the external stress σ is raised toward the yield stress σ_Y, the material responds by larger and larger dislocation avalanches, whose characteristic size diverges at σ_Y. Right at this point, the plastic strain γ would grow indefinitely. We may wonder why macroscopic deformation looks smooth if the internal strain avalanches are scale-free. An important fact is that when most materials deform, the dislocation density increases, leading to strain hardening: The stress required to sustain plastic flow increases with deformation, as if an additional back-stress $\sigma_b = -\Theta\gamma$ were building up inside the crystal (where Θ is a phenomenological coefficient). The back-stress opposes the propagation of large plastic avalanches, inducing a finite characteristic size. For this reason, we do not normally see steps in the stress-strain curves, although dislocation avalanches can still be revealed when probing small scales in acoustic emission experiments (*5*).

The scale-invariant strain bursts observed in crystal plasticity have a counterpart in ferromagnetic materials. In thin films, for instance, irregular steps in the magnetization curve can be seen by magneto-optical methods (*6*) (see the figure, top right). These steps reflect the erratic dynamics of domain walls, separating regions of opposite magnetization *M* (figure, bottom right). Domain walls are pinned by the impurities present in the material and start to move, magnetizing the sample, when the applied magnetic field *H* overcomes the coercive field H_c, in a way analogous to dislocations at the yield stress. In addition, large domain wall avalanches are hindered by dipolar interactions that induce a demagnetizing field opposed to the magnetization: $H_d = -\kappa M$ (where κ is the demagnetization factor) (*7*). Thus, hysteresis loops appear smooth in thick samples but look more irregular in thin films where κ vanishes. The close analogy between plasticity and magnetism, which are two apparently very different problems, provides a vivid illustration of the principles of complexity: Collective phenomena often obey simple rules, regardless of the distinctive details.

The experimental results presented by Dimiduk *et al*. open the way to understanding and possibly controlling fluctuations in plastic deformation. This is a topic of great technological importance in view of the current trend toward device miniaturization. Furthermore, this understanding could pave the way for a microscopic theory of the yielding transition of interacting dislocation assemblies. Although this represents a formidable task, important steps in this direction have been taken recently by Zaiser and Moretti (*8*). The theoretical conditions they study are not far from those in the experiments by Dimiduk and co-workers, and indeed the value of the experimentally measured power-law exponent (*1*) is explained by the theory (*8*). These results confirm that plasticity is an excellent playground for statistical mechanics methods and ideas.

References

1. D. M. Dimiduk *et al*., *Science* **312**, 1188 (2006).
2. M. D. Uchic *et al*., *Science* **305**, 986 (2004).
3. J. P. Sethna *et al*., *Nature* **410**, 242 (2001).
4. M.-C. Miguel *et al*., *Phys. Rev. Lett*. **89**, 165501 (2002).
5. M.-C. Miguel *et al*., *Nature* **410**, 667 (2001).
6. E. Puppin, *Phys. Rev. Lett*. **84**, 5415 (2000).
7. S. Zapperi *et al*., *Phys. Rev. B* **58**, 6563 (1998).
8. M. Zaiser, P. Moretti, *J. Stat. Mech.* 10.1088/1742-5468/2005/08/P08004 (2005).
9. M.-C.M. acknowledges financial support from Ministerio de Educación y Ciencia (Spain) and DURSI (Generalitat de Catalunya).

10.1126/science.1127729